it has been suggested[3] that the odd components of the axial crystalline field contribute importantly to the value of $D$, the arguments given are no longer considered to be valid.[18] While it is clear that such an over-simplified calculation, based as it is on a point charge model, cannot be expected to give accurate results; it nevertheless indicates that ionic motion probably plays an important role in the microwave electric field effect for $Fe^{3+}$ and $Mn^{2+}$ just as for $Cr^{3+}$. However, the above discussion does not rule out possible significant contributions from the effect of distortion of the electronic wave function of these $S$-state ions.

It would be valuable to examine ions which are iso-electronic to the more tractable $Cr^{3+}$ ion. These include $V^{2+}$ and $Mn^{4+}$ which have $D$ parameters in $Al_2O_3$ closely similar[16] to that for $Cr^{3+}$. In addition, the effect of electric fields on the optical spectra of these ions has been studied and interpreted in terms of electronic wave function distortion and ionic displacement.[19] Both of these ions are presently under study in this Laboratory.

### ACKNOWLEDGMENTS

The author would like to express his thanks to V. J. Folen for many illuminating discussions and for his help in x-ray crystal orientation, to R. A. Becker for growing the crystals used, and to the Electron Tubes Shop at the Naval Research Laboratory for their help in fabricating and silvering the samples. I also profited by discussions with J. O. Artman and J. C. Murphy and from the receipt of a copy of M. D. Sturge's manuscript prior to publication.

[18] J. O. Artman and J. C. Murphy (to be published).

[19] M. D. Sturge, Phys. Rev. **133**, A795 (1964).

# Coercive Force of Iron Resulting from the Interaction of Domain Boundaries with Large Nonmagnetic Inclusions

WILLIAM D. NIX AND ROBERT A. HUGGINS

*Department of Materials Science, Stanford University, Stanford, California*

The interaction of large inclusions with slowly moving domain boundaries has been quantitatively examined and the contribution made by such inclusions to the coercive force predicted. Several physical models of the interaction between large inclusions and moving Bloch walls were investigated by making calculations of the energy of the closure domain configuration about the inclusions for various positions of the moving domain boundary. By statistically treating a random distribution of inclusions, the coercive force was calculated as a function of the inclusion distribution parameters. Several features of the interactions between spike-shaped closure domains and moving domain boundaries have been elucidated.

## I. INTRODUCTION

IT has been shown by many investigators that dislocations, nonmagnetic inclusions, and other chemical and physical inhomogeneities influence the properties of bulk ferromagnetic materials. One manner in which imperfections affect the magnetic properties of a material is by acting as impediments or obstacles to the motion of domain boundaries. An analysis of the interaction between domain boundaries and structural imperfections is important in the understanding of irreversible ferromagnetic properties at low and intermediate frequencies.

The particular problem of the determination of the contribution to the coercive force which results from the interaction of domain boundaries with large non-magnetic inclusions is treated in this paper. It consists of an analysis of the interaction of a moving boundary with the subsidiary domain structure about such inclusions.

One of the first attempts to evaluate the effects of nonmagnetic inclusions on coercive force was that by Kersten.[1] He supposed that the binding energy between a Bloch wall and a nonmagnetic inclusion is given by the reduction in interfacial energy caused by the intersection of the particle by the domain boundary. It was shown by Néel[2] that when a Bloch wall bisects an inclusion, the reduction in the magnetostatic energy is much greater than the change in Bloch wall energy and is therefore more important in determining the binding energy. Néel[3] also later showed that it is necessary to adopt a realistic statistical model of the particle distribution to be able to compute the coercive force which arises from small inclusions. Dijkstra and Wert,[4] using a simplified form of Néel's statistical model, calculated the coercive force due to inclusions with diameters up to the thickness of a Bloch wall.

[1] M. Kersten, Physik. Z. **44**, 63 (1943).

[2] L. Néel, Cahiers Phys. **25**, 21 (1944).

[3] L. Néel, Ann. Univ. Grenoble **22**, 299 (1946).

[4] L. J. Dijkstra and C. Wert, Phys. Rev. **79**, 979 (1950).

The existence of spike-shaped closure domains about large inclusions was first predicted by Néel[2] and later directly observed by Williams.[5] Because of the presence of the subsidiary domains about such particles, it was recognized that a computation of the coercive force resulting from the presence of large inclusions must take them into account. Néel,[2] Dijkstra and Wert,[4] and Goodenough[6] developed similar models for coercive force based on the existence of the spike-shaped domains. They proposed that in the absence of other mechanisms of demagnetization, the coercive force would be equal to the critical field required for the un- limited growth of the spike-shaped domains. The values of coercive force calculated in this way are much higher than those observed.

It was shown first by Williams[7] and later by others[8,9] that the presence of the subsidiary domains around an inclusion modifies the interaction of that inclusion with a migrating Bloch wall. From this observation it became clear that models for the coercive force due to large inclusions should be based on the interaction of the subsidiary domains with moving boundaries. Further evidence of the existence and behavior of Néel spikes has been obtained in ferrite materials.[10]

Since the observations of Williams played a central role in the formulation of several theories relating coercive force to large nonmagnetic inclusions, it deserves brief mention here. He observed that when a Bloch wall approaches an inclusion and its Néel spikes, the spikes make contact with the wall and become tapered tubes connecting the inclusion to the migrating Bloch wall. As the wall moves toward the inclusion, the tube domains become shorter and finally disappear when the wall bisects the inclusion. When the wall migrates away from the inclusion, tube domains are re-established between the inclusions and the wall. Finally, as the moving wall pulls further away from the inclusion the tube domains leave the wall and snap back to a spike-shaped configuration. This "snapping" process which accompanies the escape of the moving wall has been studied experimentally by Bates and Carey[8,9] and theoretically by Brenner.[11] Their results indicate that the tube domains extend approximately 40% be- fore the wall breaks free.

Kondorsky[12] and Kersten[13] have independently established rather similar models for the coercive force which results from the interaction between the closure

domains of an inclusion and a moving Bloch wall. Both of these treatments suppose that the coercive force is that field for which a Bloch wall can be pulled away from the tube domains connecting it with the inclusion. While there is no doubt that the tube domains retard the motion of the receding Bloch wall, the snap- ping process which accompanies the escape of the Bloch wall may not be the most significant part of the inter- action in determining the coercive force. The results of the calculations reported in this paper will indicate that the "snapping" process plays a rather insignificant part in the determination of the binding energy of a Bloch wall to a large inclusion. It should also be pointed out that the calculations by both Kersten and Kon- dorsky were not based on a statistically random distri- bution of inclusions. Instead, they assumed a specific ordered arrangement.

## II. THEORY

From the observations reported in the previous section it is clear that a model for the coercive force of materials having large inclusions must include a detailed analysis of the behavior of their associated domain structure. In addition, a realistic treatment of the particle distribution must be utilized.

The approach which has been adopted in these cal- culations involves the determination of the energy pro- file related to the position of a Bloch wall as it passes and interacts with an inclusion and its subsidiary domain structure. It will be shown that these energy profiles can be characterized by parameters which, through a statistical model, lead directly to a calculation of coercive force.

The initial stage of all interactions is assumed to be characterized by a planar Bloch wall which is migrating toward an inclusion. Before the Bloch wall has reached the extremities of the subsidiary domain structure, the energy of the system is given by the equilibrium energy of the unperturbed closure domain structure about the inclusion. As the Bloch wall moves closer to the particle, a reaction occurs such that the equilibrium closure domain structure is altered. The energy of the system can be determined by finding that domain configuration for which the total magnetic energy is a minimum. By making a computation of the minimum energy of the system for all positions of the migrating wall, it is possi- ble to determine the energy profile related to the wall position. When the moving wall has passed the inclusion and is no longer interacting with the spike-shaped domains, the energy of the system returns to the initial value corresponding to the equilibrium structure of the closure domains about the inclusion.

### Physical Model for the Interactions

As in most calculations dealing with domain con- figurations, it is assumed that the magnetization of each domain lies along an easy crystallographic direction

[5] H. J. Williams, Phys. Rev. **71**, 646 (1947).
[6] J. B. Goodenough, Phys. Rev. **95**, 917 (1954).
[7] H. J. Williams (unpublished) cited in: C. Kittel and J. K. Galt, Ref. 10, p. 530.
[8] L. F. Bates and R. Carey, Proc. Phys. Soc. (London) **75**, 880 (1960).
[9] L. F. Bates and R. Carey, Proc. Phys. Soc. (London) **76**, 754 (1960).
[10] C. Kittel and J. K. Galt, in *Solid State Physics*, edited by F. Seitz and D. Turnbull (Academic Press Inc., New York, 1956), Vol. 3, p. 538.
[11] R. Brenner, Z. Angew. Phys. **7**, 391 (1955).
[12] E. Kondorsky, Dokl. Akad. Nauk SSSR **68**, 37 (1949).
[13] M. Kersten, Z. Angew. Phys. **7**, 397 (1955).

and is not perturbed from that direction by the application of an external magnetic field. Implicit in this assumption is the supposition that the crystal anisotropy energy and the exchange energy of a domain configuration can be accounted for by computing the interfacial energies of all of the Bloch walls in the configuration.

It has been assumed that the inclusions may be treated as cubic having edges which lie parallel and perpendicular to $\langle 100 \rangle$ directions in the cubic lattice. Since the thickness of a Bloch wall is approximately 0.1 $\mu$, it is expected that this calculation is valid only for particles larger than one micron in diameter.

One of the important additional assumptions made in this treatment relates to the condition of reversibility which is assumed for all reactions. It was assumed that the migrating Bloch wall moves slowly enough that the domain configurations do not differ significantly from equilibrium configurations. It has also been supposed that the nucleation of reverse domains, when expected from total magnetic energy considerations, occurs with sufficient ease that equilibrium is maintained at all times.

## Basic Equations

The factors which determine the total magnetic energy of a given domain configuration are (1) Bloch wall energy, (2) magnetostatic energy, and (3) magnetostrictive energy

The calculation of the total Bloch wall energy in a complex configuration involves an account of the total Bloch wall area as well as a knowledge of the interfacial energies of the boundaries which compose the configuration. The following interfacial energies, which have been determined theoretically[14,15] and which are in general agreement with those obtained by experiment,[16] were used in these calculations: (1) $\sigma_{(180tw)}$ = 1.8 ergs/cm²; (2) $\sigma_{(90tw)}$ = 0.9 ergs/cm²; (3) $\sigma_{(90tl)}$ = 1.5 ergs/cm².

The magnetostrictive energy per unit volume for iron is given by

$$w_{ms} = \tfrac{1}{2} Y \epsilon^2 , \qquad (1)$$

where $Y$ is the elastic modulus, equal to $2 \times 10^{12}$ dynes/cm² and $\epsilon$ is the magnetostriction constant, given by Carr[17] as $32 \times 10^{-6}$. The magnetostrictive energy of a domain configuration is found from this equation by computing the total volume of the domains whose magnetization is normal to the magnetization of their environment.

An accurate calculation of the magnetostatic energy

[14] L. Néel, Cahiers Phys. 25, 1 (1944).
[15] K. H. Stewart, *Ferromagnetic Domains* (Cambridge University Press, London, 1954), p. 99.
[16] L. F. Bates and P. F. Davis, Proc. Phys. Soc. (London) 74, 170 (1959).
[17] W. J. Carr, Jr., *Magnetic Properties of Metals and Alloys* (American Society for Metals, Cleveland, 1959), p. 200.
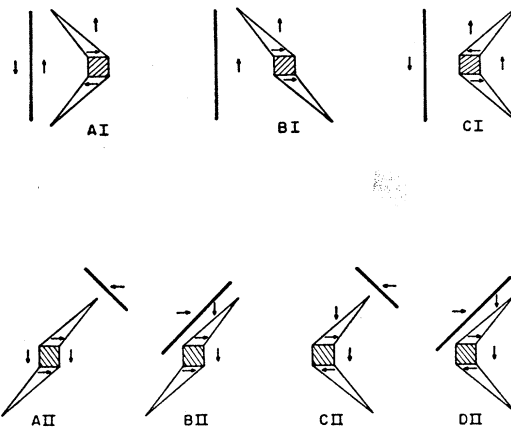
FIG. 1. Potential interactions between both 180° and 90° Bloch walls and the spike-shaped domains about nonmagnetic inclusions.

of a system can only be made for very simple geometric shapes. However, an approximate method which can be used in problems relating to domain configurations, was suggested by Kittel.[18] It involves the supposition that the magnetostatic energy can be treated as an interfacial wall energy term applicable to Bloch walls exhibiting a uniform distribution of magnetic poles. The density of magnetic poles on a Bloch wall is given by $4\pi(M_1 - M_2)$, where $M_1$ and $M_2$ represent the normal components of the intensity of magnetization in the adjacent domains. The magnetostatic component of the interfacial energy is expressed as

$$\sigma_{mag} = 2\pi(M_1 - M_2)^2 d , \qquad (2)$$

where $d$ is the thickness of the wall. The total magnetostatic energy of a domain configuration is computed with this equation by determining the magnetic pole distribution on each of the Bloch walls in the configuration.

## Statistical Model for Coercive Force

The basis of the statistical treatment used in this paper was first described by Néel[3] and later modified and simplified by Dijkstra and Wert.[4]

Consider a single domain, cubic in shape and having a dimension $L$. A single Bloch wall residing within the domain is positioned at $Z = Z_0$. Because of the interaction between the inclusions within the domain and the isolated boundary, one may state that the total energy of a given domain varies in an irregular manner with the position of the moving wall. Néel suggested that the irregular energy profile can be approximated by a polygonal contour having a fixed number of sides. When a wall is in an equilibrium position, the force exerted on the wall by the application of an applied magnetic field $H(Z_0)$ is balanced by the forces exerted on that wall by the various inclusions and their subsidiary domain structures. Since the total force exerted on a single Bloch wall

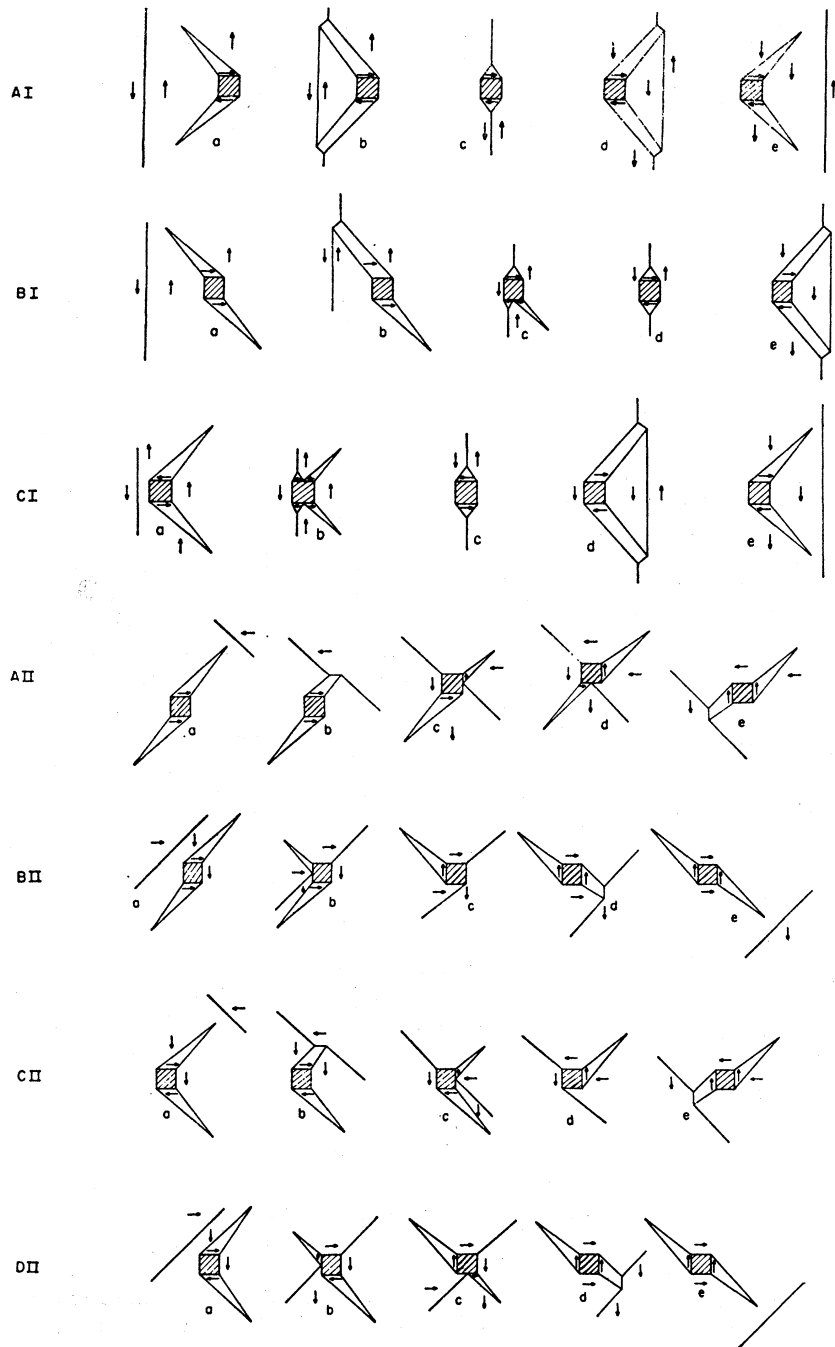[18] C. Kittel, Rev. Mod. Phys. 21, 541 (1949).

FIG. 2. Sequence of domain configurations which arise as a result of the interaction of a large inclusion with a moving Bloch wall.

by the external field is given as $2H(Z_0)M_sL^2$,[2] the force balance for the wall is expressed as

$$2H(Z_0)M_sL^2 = \sum_i (\partial/\partial Z_0)[\varphi(Z_i - Z_0)], \qquad (3)$$

where $M_s$ is the saturation magnetization, $Z_i$ is the coordinate position of the $i$th inclusion and $\varphi(Z_i - Z_0)$ is the decrement in the energy of the system, which arises from the interaction of the wall with the $i$th inclusion.

Inasmuch as the energy profiles within each domain in a real material are not identical, the coercive force is given by

$$H_c = \langle H_m^2 \rangle_{av}^{1/2}, \qquad (4)$$

where $H_m$ corresponds to the steepest energy gradient in each domain and the average is taken over all the domains in a bulk sample. Following Néel,[19]

$$\langle H_m^2 \rangle_{av} = 2\langle H^2(Z_0) \rangle \ln p, \qquad (5)$$

[19] L. Néel, Cahier Phys. 12, 1 (1942).

where $\langle H^2(Z_0)\rangle$ is the mean value of $H^2(Z_0)$ taken over all values of $Z_0$ within a domain, and $p$ is the number of sides of the polygonal energy contour. Since a Bloch wall interacts with inclusions which are located within a small distance $\frac{1}{2}\delta$ from the wall, it follows that the polygonal parameter, $p$, can be approximated as

$$p = 2L/\delta. \qquad (6)$$

Following the statistical argument given by Dijkstra and Wert,[4] Eq. (3) yields

$$\langle H^2(Z_0)\rangle = \frac{n\int_\delta \left\{\frac{\partial}{\partial Z_0}[\varphi(Z-Z_0)]\right\} dZ}{4M_s^2 L^2}, \qquad (7)$$

where $n$ is the number of inclusions per unit volume. Letting $\alpha$ be the volume fraction of inclusions and $a$ be the inclusion dimension, we have

$$n = \alpha/a^3. \qquad (8)$$

Equations (4)–(8) give

$$H_c = \left[\frac{\alpha\int_\delta \left\{\frac{\partial}{\partial Z_0}[\varphi(Z-Z_0)]\right\}^2 dZ \ln\left(\frac{2L}{\delta}\right)}{2M_s^2 L^2 a^3}\right]^{1/2}, \qquad (9)$$

where $\delta$ is the distance through which the moving domain boundary interacts with a stationary inclusion. By letting

$$\Delta\varphi_I = \int_\delta \left\{\frac{\partial}{\partial Z_0}[\varphi(Z-Z_0)]\right\}^2 dZ, \qquad (10)$$

the coercive force becomes

$$H_c = \left[\frac{\alpha\Delta\varphi_I \ln\left(\frac{2L}{\delta}\right)}{2M_s^2 L^2 a^3}\right]^{1/2}. \qquad (11)$$

In order to compute the magnitude of the coercive force it is therefore necessary to determine the parameters $\Delta\varphi_I$ and $\delta$. With these parameters the coercive force can be determined from Eq. (11) as a function of the average domain size $L$, and the inclusion parameters $\alpha$ and $a$.

### III. MODELS

In all, there are seven distinct types of interactions that involve spike-shaped domains and either 180° or 90° Bloch walls. These are illustrated in Fig. 1. Each of these interactions has been treated separately and characterized by values of the interaction parameters $\Delta\varphi_I$ and $\delta$.

Figure 2 illustrates the sequence of domain configurations which arise during each of the seven interactions.

The energy profiles, from which the interaction parameters are obtained, have been determined by computing the total magnetic energy as a function of Bloch wall position by means of the equations given in the previous section. To a large extent, the calculations are simple geometrical computations but which, nevertheless, are tedious and best handled by an automatic digital computer. In two instances, unique features of the interactions must be treated with special consideration.

Consider the blunt spike domain configuration which appears in Fig. 2. The driving force for the formation of the blunted spike domain is the reduction in magnetostatic energy associated with free magnetic poles on the surfaces of a pointed Néel spike. As the tubular domain becomes more blunt, the surfaces become more nearly parallel, and the magnetostatic energy is significantly reduced. Because of the disturbance at the end of the blunt spikes, the moving wall is no longer planar. This particular deviation causes magnetic charges to be distributed on the moving wall as well, and gives rise to an associated increment in the total magnetostatic energy. It follows that the equilibrium configuration is given by the minimum total energy, which involves a compromise between the magnetostatic energy of the 90° tilt walls and the magnetostatic energy of the moving Bloch wall.

When a moving Bloch wall first interacts with a spike-shaped domain at the particle-closure domain interface, a special feature is developed. This feature is displayed by the interaction C I, which is illustrated in Fig. 2. As the wall moves across the inclusion, the spike-shaped closure domain is slowly eliminated and replaced by a newly-formed closure domain. This process was treated quantitatively by applying the results of a previous calculation[20] in slightly modified form.

### IV. RESULTS AND DISCUSSION

The details of the quantitative treatment will not be given here, since the can be found elsewhere.[21]

Energy profiles for each of the seven interactions for the case of a 1-$\mu$ particle are given in Figs. 3 and 4. The interaction parameters $\Delta\varphi_I$ and $\delta$ are given in Table I. Typical values for coercive force calculated from Eq. (11) are given in Table II.

A direct comparison of the calculated values of coercive force with experimental values can only be made when the inclusion volume fraction, domain size and inclusion size have all been simultaneously measured. No such data are yet available. While the coercive force data of Dijkstra and Wert[4] are applicable only to small inclusions, they represent values to which ex-

[20] W. D. Nix and R. A. Huggins, Phys. Rev. 121, 1038 (1961). Errata: The value of the constant $P$ for a 0.5-$\mu$ inclusion should be changed to $0.578\times10^{-9}$. Graphical representation of the functions are erroneous as a result. The problem has since been solved more concisely. (See Ref. 21.)

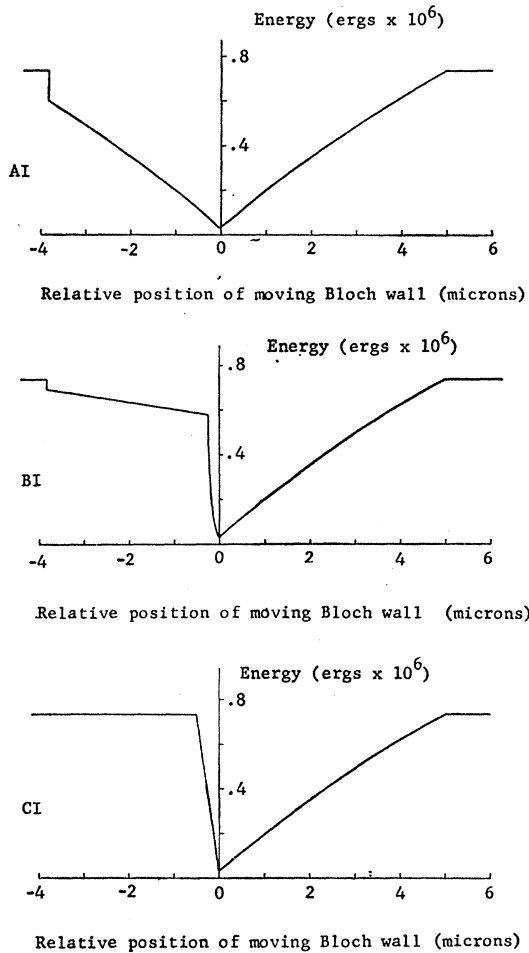[21] W. D. Nix, Ph.D. dissertation, Stanford University, 1963 (unpublished).

Relative position of moving Bloch wall (microns)



Relative position of moving Bloch wall (microns)



Relative position of moving Bloch wall (microns)

FIG. 3. Energy profiles for the interactions involving 180° Bloch walls for a 1-$\mu$ inclusion.

TABLE II. Compilation of values of coercive force for several values of the inclusion size $a$ and volume fraction $\alpha$ for a domain size $L=5\times10^{-3}$ cm.

| Inclusion volume fraction | Coercive force | Inclusion size (microns) | | | |
|---|---|---|---|---|---|
| | | 1.0 | 2.0 | 4.0 | 8.0 |
| $\alpha=1.0\times10^{-3}$; | $H_c$[a] | 0.36 | 0.32 | 0.24 | 0.14 |
| $\alpha=5.0\times10^{-3}$; | $H_c$ | 0.84 | 0.72 | 0.56 | 0.32 |
| $\alpha=1.0\times10^{-2}$; | $H_c$ | 1.20 | 1.02 | 0.78 | 0.44 |
| $\alpha=5.0\times10^{-2}$; | $H_c$ | 2.68 | 2.26 | 1.76 | 1.00 |
| $\alpha=1.0\times10^{-1}$; | $H_c$ | 3.78 | 3.20 | 2.50 | 1.40 |

[a] $H_c$ in oersteds.

pressions for large inclusions must extrapolate. For $\alpha=3\times10^{-3}$ and $a=1.0$ $\mu$, the Dijkstra and Wert data extrapolate to 0.5 Oe whereas Eq. (11) yields 0.4 Oe. This calculated value is obtained by assuming a domain size of $10^{-2}$ cm and by taking an average of the coercive force values found for each of the seven possible interactions.

From the energy profiles shown in Figs. 3 and 4 it is clear that the binding energy between the moving wall
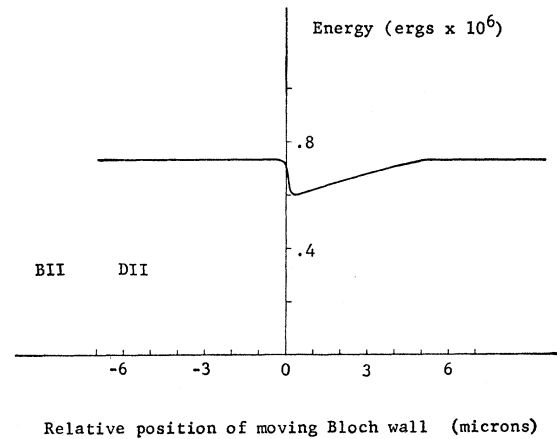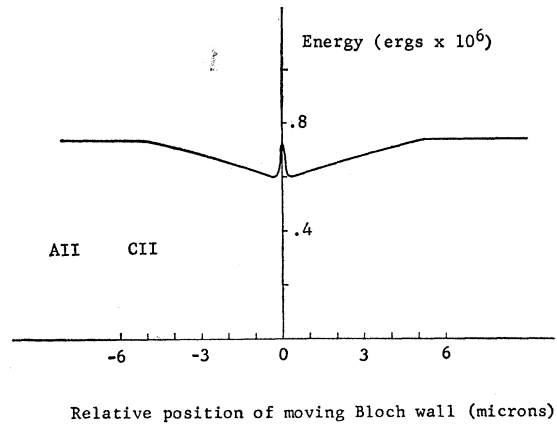
TABLE I. Compilation of the interaction parameters $\Delta\varphi_I$ and $\delta$ for several inclusion sizes for each of the seven distinct interactions described in Fig. 1.

| Inter-action | Interaction parameters[a] | Inclusion size (microns) | | | |
|---|---|---|---|---|---|
| | | 1.0 | 2.0 | 4.0 | 8.0 |
| A I | $\Delta\varphi_I$ | $1.9\times10^{-9}$ | $1.6\times10^{-8}$ | $1.3\times10^{-7}$ | $1.1\times10^{-6}$ |
| | $\delta$ | 9.4 | 18.8 | 37.5 | 74.6 |
| B I | $\Delta\varphi_I$ | $1.1\times10^{-8}$ | $8.4\times10^{-8}$ | $6.8\times10^{-7}$ | $5.6\times10^{-6}$ |
| | $\delta$ | 9.4 | 18.8 | 37.5 | 74.6 |
| C I | $\Delta\varphi_I$ | $1.2\times10^{-8}$ | $9.8\times10^{-8}$ | $8.0\times10^{-7}$ | $6.7\times10^{-6}$ |
| | $\delta$ | 5.9 | 11.9 | 23.8 | 47.6 |
| A II | $\Delta\varphi_I$ | $2.2\times10^{-9}$ | $1.7\times10^{-8}$ | $1.5\times10^{-7}$ | $1.3\times10^{-6}$ |
| | $\delta$ | 12.5 | 24.9 | 49.8 | 97.6 |
| B II | $\Delta\varphi_I$ | $3.2\times10^{-9}$ | $2.5\times10^{-8}$ | $2.2\times10^{-7}$ | $2.5\times10^{-6}$ |
| | $\delta$ | 7.1 | 14.1 | 28.2 | 56.4 |
| C II | $\Delta\varphi_I$ | $2.2\times10^{-9}$ | $1.7\times10^{-8}$ | $1.5\times10^{-7}$ | $1.3\times10^{-6}$ |
| | $\delta$ | 12.5 | 24.9 | 49.8 | 97.6 |
| D II | $\Delta\varphi_I$ | $3.2\times10^{-9}$ | $2.5\times10^{-8}$ | $2.2\times10^{-7}$ | $2.5\times10^{-6}$ |
| | $\delta$ | 7.1 | 14.1 | 28.2 | 56.4 |

[a] $\Delta\varphi_I$ in ergs$^2$cm$^{-1}$; $\delta$ in microns.



Relative position of moving Bloch wall (microns)



Relative position of moving Bloch wall (microns)

FIG. 4. Energy profiles for the interactions involving 90° Bloch walls for a 1-$\mu$ inclusion.
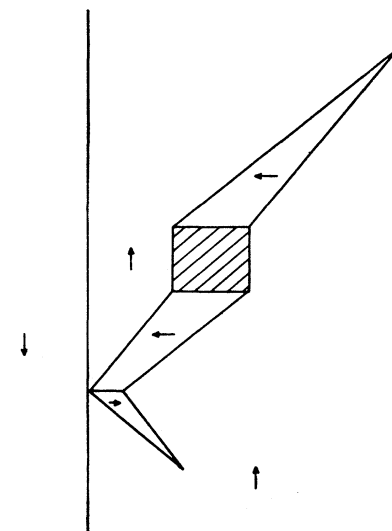
and the inclusion is much greater when the wall is near the inclusion, especially for 180° walls. It also follows that the parameter, $\Delta\varphi_I$, which characterizes the binding energy in Eq. (11), is related more to the behavior near the inclusion than to the processes which occur when the wall is pulling free from the clinging tubular domains. This result indicates that while the snapping process should occur, it does not play as central a role in the determination of coercive force as has been proposed.[12,13]

Examination of the energy profiles indicates that the tubular domains extend approximately 40% before breaking free from the moving wall. This result is consistent with experimental observations.[8]

Another important feature of the interaction between moving Bloch walls and large inclusions concerns the transformation of the spike domain structure from one form to another. When a 180° wall passes a large inclusion, the subsidiary domain structure is transformed into one in which the magnetization vectors of the two spike domains are antiparallel, regardless of the nature of the existing domain structure before the interaction. The interaction with 90° walls, on the other hand, causes the domain structure to be converted into a form in which the magnetization vectors of the two spike-shaped domains are parallel. Some implications of this observation can be found elsewhere.[22]

As can be seen from Figs. 3 and 4, the major difference between the interaction of large inclusions with 180° walls and 90° walls involves the absence of the deep energy well in the case of 90° walls. Because of the relative orientation of 90° walls with the spike-shaped domains, it is impossible to completely eliminate both of the closure domains at the same stage of the interaction. For this reason, the migrating 90° wall is less tightly bound to the inclusion and, therefore, can more easily escape. Because of the weak binding for the case of 90° walls, one would expect a correspondingly small probability that particles will have a significant influence on the motion of such walls. This particular observation gives a physical explanation of the experimental fact that 90° walls do not cause Barkhausen discontinuities.[23] A 180° wall, on the other hand, must

---

[22] W. D. Nix and R. A. Huggins (to be published).
[23] R. S. Tebble, Proc. Phys. Soc. (London) **B68**, 1017 (1955).



FIG. 5. Development of a fold in a Néel spike due to the presence of a 180° Bloch wall.

negotiate a deep energy wall as it interacts with each large inclusion and can, therefore, cause Barkhausen discontinuities.

An aberration in the perfect spike-shaped domain structure which is occasionally observed is shown in Fig. 5. This work suggests a possible cause for the formation of such a configuration. From the quantitative treatment described one can show that when a moving wall encounters the sharp end of a Néel spike, the energy of that system is only slightly diminished by the formation of a blunt tubular domain. It is therefore possible that under some special circumstances, the energy of the blunt configuration may be slightly greater than that of the pointed shape. In such a case the energy of the domain configuration could be reduced by the formation of a fold in the Néel spike, as illustrated in Fig. 5.

## ACKNOWLEDGMENTS